JOURNAL OF MATERIALS SCIENCE. MATERIALS IN MEDICINE 5 (1994) 411–416

Bone ingrowth analysis and interface evaluation of hydroxyapatite coated versus uncoated titanium porous bone implants

A. MORONI*, V. L. CAJA, C. SABATO
Third Department of Orthopaedic Surgrey, Rizzoli Orthopaedic Institute, Via G. C. Pupilli 1, 40136 Bologna, Italy

E. L. EGGER, F. GOTTSAUNER-WOLF, E. Y. S. CHAO
Orthopaedic Biomechanics Lab., Department of Orthopaedics, Mayo Clinic, Mayo Foundation, Rochester Minnesota, USA

Fourteen titanium porous-coated implants with a cylindrical shape (length 22 mm and diameter 5±0.3 mm) were prepared. Bead size was 250–350 μm. Seven implants were plasma-sprayed with hydroxyapatite and the other seven remained uncoated. Implants, both hydroxyapatite-coated and uncoated, were randomly selected and press fitted longitudinally into the proximal femoral cancellous bone bilaterally in seven dogs. After 12 weeks the dogs were euthanized and push-out and histomorphometric backscattered electron microscopy studies were carried out. No statistical differences in the mechanical tests were observed. Comparing hydroxyapatite-coated versus uncoated implants, the histomorphometric results showed statistical significance in the percentage of bone ($p=0.01$); and in bone index, ratio between bone ingrowth and bone ongrowth ($p=0.01$). The size of the bone implant interface was smaller in the hydroxyapatite-coated implants than in the uncoated ($p=0.029$). Beneficial effects of hydroxyapatite applied to spherical bead titanium porous coatings were demonstrated. These morphological and histomorphometric results support the concepts involved with the use of hydroxyapatite as a coating for uncemented porous prosthetic devices.

1. Introduction

The attachment strength of the bone–prosthesis interface is a very important issue affecting the clinical outcome of total joint replacements [1–5]. Biological fixation of uncemented prostheses can be obtained by bone formation within a porous coating or macrotextured metallic surface [6–8]. Of the materials used to obtain a porous coating, titanium alloy is very attractive due to its high strength, comparatively low elastic modulus, light weight and resistance to corrosion. Synthetic hydroxyapatite has shown the ability to bind chemically to the bone. Recently hydroxyapatite plasma-spray coating of titanium prostheses has been proposed as a suitable method to enhance the bone fixation of uncemented prostheses [9, 10].

Different animal models have shown greater surface bonding strength when hydroxyapatite-coated implants were compared to uncoated after cortical bone implantation [11–16]. However, there is little information on osteoconductive capacity and interface strength when hydroxyapatite-coated titanium porous-coated implants are used in a noncortical model

The purpose of this study was to compare the biological and biomechanical responses in a group of titanium porous-coated implants with and without hydroxyapatite coating in a canine femoral cancellous bone model.

2. Materials and methods

2.1. Implant characteristics

Fourteen titanium porous-coated implants with a cylindrical shape (length 22 mm and diameter 5 ± 0.3 mm) were manufactured by De Puy USA (Warsaw, Indiana 45680). Bead diameter was 250–350 μm and the number of bead layers was 3–4. The porosity before hydroxyapatite coating, calculated using backscattered electron microscopy, was 47.3 ± 5.6%. Seven samples were plasma-sprayed with hydroxyapatite (Biocoatings, Flametal, Fornovo Taro, Italy), and the remaining seven remained uncoated. The outer bead layer was entirely coated by hydroxyapatite. In contrast, the inner bead layers were only partially coated by hydroxyapatite. The cristallinity ratio of hydroxyapatite, calculated after X-ray spectroscopy, was more than 70%, and purity by mass spectroscopy, more than 97%. The Ca/P ratio was 1.67 ± 0.01. The thickness of the hydroxyapatite coating was 30–60 μm. The hydroxyapatite powder presented small traces of heavy elements below the limits set by the ASTM F1185–88 standard test (As < 2 ppm; Cd < 1 ppm; Hg < 1 ppm; Pb < 1 ppm;

* To whom correspondence should be addressed.

0957–4530

total heavy elements < 30 ppm; Cu < 1 ppm; Mn < 100 ppm; Fe < 100 ppm).

2.2. Surgical technique

Seven adult mixed-breed dogs of similar size and weight (25 kg average) were used. Maturity was determined by radiographic examination of the physes of the proximal tibia and distal femora to confirm closure. General anesthesia was induced and maintained with intravenous pentobarbital sodium (55–65 mg kg^{-1}). Perioperative antibiotics (Cefazolin 22 mg kg^{-1}) were given starting the day before surgery, for 3 days. Both hind limbs were clipped, the animals placed in lateral recumbency, and both limbs aseptically prepared and draped for surgery.

Implants, both hydroxyapatite-coated and uncoated, were randomly selected and press-fitted longitudinally into the proximal femoral cancellous bone bilaterally in seven dogs (Fig. 1). The greater trochanter was approached through a dorsal incision, the superficial gluteal and middle gluteal muscles were tenotomized. The external rotator muscles were likewise incised to expose the trochanteric fossa. A 3.5 mm diameter drill was advanced down the proximal shaft of the femur to a depth of 22 mm. The hole was reamed to a diameter 0.2 mm smaller than the sample to implant. Individual reamers were used for each implant in order to achieve a press-fit implantation in a consistent manner, independent of the implant diameter variations. Implants were press-fitted into these holes to lie in the cancellous bone medullary canal on the longitudinal axis of the femur.

Following surgery, the dogs were placed in recovery rooms in heated cages and closely monitored over 24 h. Butorphanol (0.4 to 0.8 mg kg^{-1} i.m.) was given for pain relief during this period. Twenty-four hours after recovery the dogs were returned to regular housing facilities where they were monitored twice a day and allowed normal activity. Implant evaluation was performed radiographically, and the animals were euthanized 12 weeks after surgery.

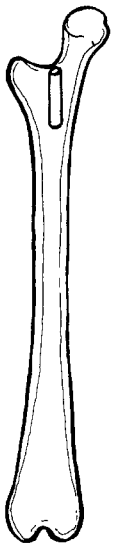

Figure 1 Site of sample implantation.

2.3. Push-out tests

One bone block from each femur, containing the implant, was studied radiographically in different projections, in order to identify the implant axes. Specimen ends were first identified by careful bone sectioning until the longitudinal axis of the implant was located.

Each block was cut four times perpendicularly to the longitudinal axis of the implant in order to obtain three middle samples from each implant discarding the end sections. Two of three samples, approximately 3 mm thick, were used for the push-out tests while the remaining sample from each implant was saved for histomorphometry. Sections were cut relatively thin to minimize the specimen alignment problem.

Each push-out specimen was centred over a 7 mm hole in an aluminum flat plate. A flat and circular plug, 5 mm in diameter was used for the push-out of the implant from the surrounding cancellous bone using an electro-mechanical universal testing machine (Instron Corporation, Canton, MA, USA) at a rate of 2 mm min^{-1}. The plug was carefully placed so that it covered the entire implant cross-section in order to obtain accurate push-out force reflecting the shear strength of the implant–bone interface.

2.4. Morphological evaluations

After the biomechanical tests, the pushed-out samples were embedded in methylmetacrylate and processed for undecalcified sectioning. Longitudinal sections were cut with a diamond saw (Leco Vari-cut VC50, USA; No. 11–4245 diamond wafering blade) to 200–300 μm thickness. After being ground to 100 μm thickness, sections were obtained and polished with alumina powder. Microradiographs of each section were performed using a standard technique, to qualitatively evaluate the morphology and the failure mechanism.

One thin slide (200–300 μm) from each unloaded section was grounded to 100 μm and coated with carbon for backscattered electron imaging (BEI). Images were created using a JSM 6400 backscattered scanning electron microscope (SEM) (JEOL Ltd. Tokyo, Japan) at 39 mm focal distance. Photographs

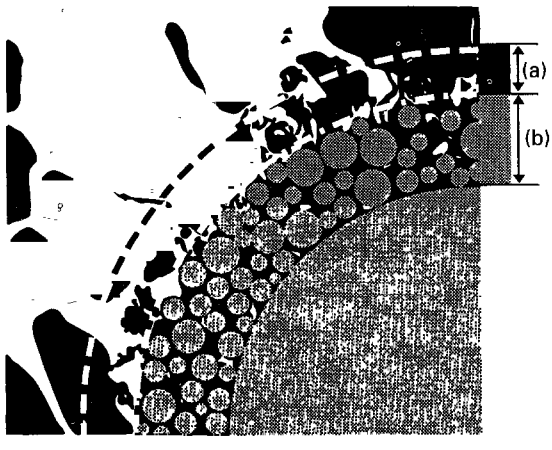

Figure 2 Representation of the histomorphometric areas. Ingrowth area thickness (a) is 500 μm and ongrowth area thickness (b) is 220 μm.

were taken at X30 or higher magnification. Histomorphometric analysis was performed using a Merz grid, with 584 points in the ingrowth area and 236 points in the ongrowth area, in the X30 magnification images. The "ingrowth area" was defined as the section area of a radial distance of 500 μm extending from the substrate, and the "ongrowth area" was defined as the section area between 500 μm and 720 μm from the substrate. Percentage of bone represents the amount of bone in the ingrowth area, and bone ingrowth represents the same quantity, but refers to the available space in the available ingrowth area. The porosity of the ingrowth area was defined as the ratio of the available area for bone ingrowth versus the "ingrowth area", in percentage. Bone ongrowth expressed the amount of bone within the "ongrowth area", in percentage. The bone index was calculated by dividing the bone ingrowth amount by the bone ongrowth amount. In addition, the depth of bone penetration was measured in twelve different locations for each sample and described as the percentage of bone penetration distance within the 500 μm "bone ingrowth" radial distance from the substrate.

At the X1000 magnification, one field with good bone–implant contact was selected, and the quality of the interface was studied by defining five materials: bone, artifactual spaces, background tissue, hydroxyapatite and titanium. In the X10 000 magnification images, the interface gap was measured every micrometre and at least ten measurements were obtained from each specimen.

2.5. Statistical evaluation

Comparison was limited to coated versus uncoated samples and was performed by two-tailed Student's t-test at a $p < 0.05$ significance value. Correlation coefficients were calculated for the push-out and histomorphometric results to establish the existence of any correlation among them.

3. Results

All animals did well after surgery, and there were no complications. The entire group of animals survived the experimental period. Implant evaluation was assessed radiographically, and there was no sign of loosening or other abnormal osseous reactions around the implants.

3.1. Push-out results

The mean push-out strength was 6.4 ± 3 MPa in the uncoated samples and 7.2 ± 3 MPa in the hydroxyapatite-coated samples ($p = 0.40$). Thus interface mechanical strength did not show statistically significant differences between hydroxyapatite-coated and uncoated implants. Likewise, no differences were found when these force data were normalized to take into account either the implant diameter, test section thickness, or calculated implant–bone interface area. Microradiographic images of the pushed-out samples showed that failure occurred mostly in the trabecular bone near the porous surface in all samples (Fig. 3).

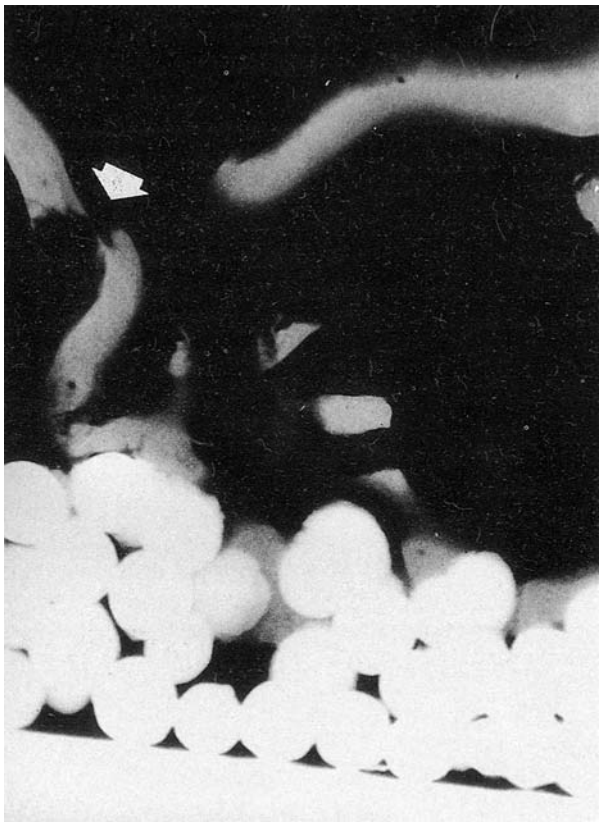

Figure 3 Microradiograph of a hydroxyapatite-coated sample after push-out test (100 μm thickness, X40). The arrow shows a trabecular fracture.

Trabecular fractures and detachments at the bone–implant interface were observed in the uncoated samples.

Debonding of hydroxyapatite coating from titanium substrate and occasionally disruptions within the hydroxyapatite surface layer were visible in hydroxyapatite-coated samples. No failure of the bone hydroxyapatite interface was observed. Hydroxyapatite coating was well present on the beads surface.

3.2. Histomorphometric results

A different morphology of the trabeculae was observed using BEI-SEM in the hydroxyapatite-coated samples compared to the uncoated ones. In uncoated samples trabeculae close to the implant surface demonstrated an arc shape with an incomplete contact pattern with the titanium surfaces (Fig. 4). In the hydroxyapatite-coated specimens, trabeculae exhibited a mushroom-like pattern with a complete and much larger contact area with the implant (Figs 5, 6). Osteocyte lacunae and vascular cavities were observed in close proximity to both the hydroxyapatite-coated and uncoated beads. Lacunae were identified as generally ovoid and 10 μm long spaces, while vascular spaces were more round and ranged from 5–70 μm in size. Histomorphometry showed a significant increase for bone percentage ($p = 0.01$) and for bone index ($p = 0.01$) in the hydroxyapatite-coated samples compared to the uncoated samples (Table I). At X1000 magnification, hydroxyapatite appeared as fragmented and bone existed in between. Artifacts were easily

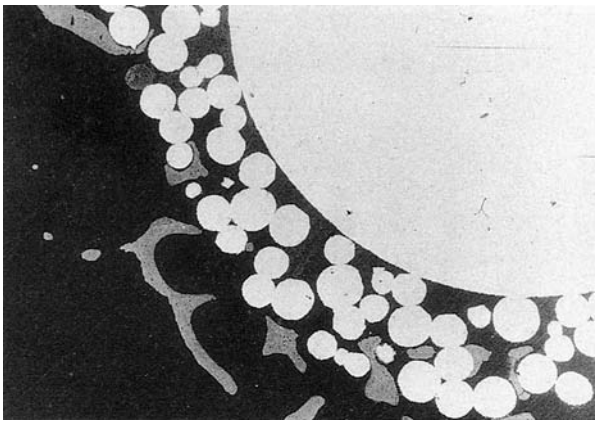

Figure 4 BEI-SEM of an uncoated sample, X30. Thin arc shape trabeculae with incomplete contact with the titanium surface can be seen.

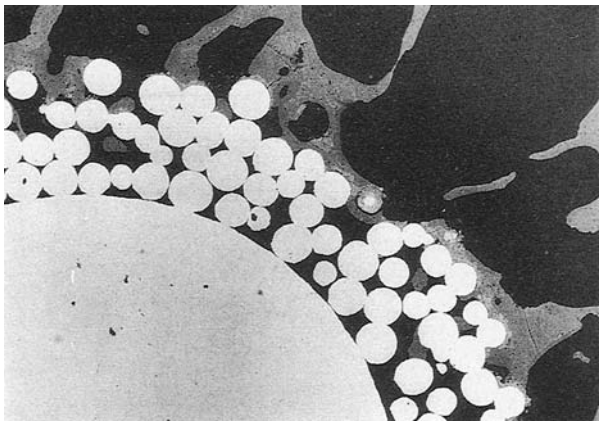

Figure 5 BEI-SEM of a hydroxyapatite-coated sample, X30. Hydroxyapatite appears as a fine coating on beaded surface. Broad mushroom-like trabeculae are visible.

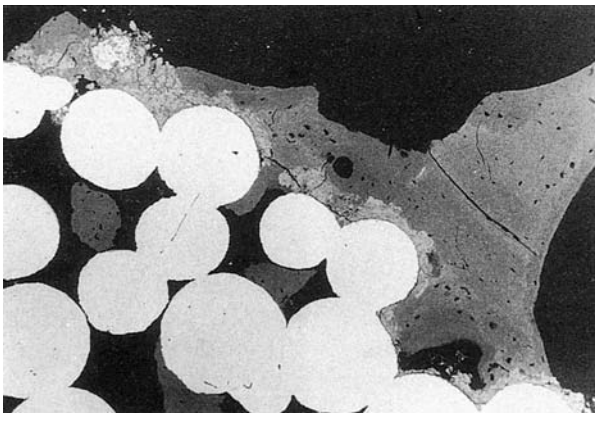

Figure 6 BEI-SEM of a hydroxyapatite-coated sample, X95. Intimate contact between a broad mushroom shape trabeculae and the implant hydroxyapatite-coated surface is shown.

distinguished in both hydroxyapatite-coated and uncoated specimens. At X10000 magnification, full contact was observed in eleven hydroxyapatite-coated specimens and in none of the uncoated specimens.

TABLE I Interface strength and histomorphometric results (mean ± SD values; $N = 7$)

Parameter	No HA	HA	p
Push-out strength (MPa)	6.4 ± 3	7.2 ± 3	0.40
Bone (%)	11 ± 4	16 ± 3	0.01
Bone ingrowth (%)	25 ± 9	33 ± 4	0.06
Porosity (%)	45 ± 5	50 ± 6	0.14
Bone ongrowth (%)	25 ± 8	21 ± 6	0.29
Bone index	98 ± 20	168 ± 7	0.01
Penetration (%)	34 ± 13	45 ± 9	0.18

TABLE II Correlation coefficient values between interface strength and histomorphometric values ($N = 7$ in all parameters)

	Percentage of bone	Bone ingrowth	Bone index	Bone depth penetration
Uncoated	0.59	0.74	0.64	0.43
Ha-coated	0.11	− 0.23	− 0.46	0.44

Measurements of the interface gap showed a significantly smaller size in the hydroxyapatite-coated specimens than in the uncoated specimens ($p = 0.029$).

3.3. Correlation between bone ingrowth and push-out strength

The correlation coefficients between push-out and histomorphometric values are shown in Table II. Bone ingrowth shows a strong correlation with push-out strength in the uncoated implants. As a consequence, all related parameters (bone percentage and bone index) showed similar correlation coefficient values. In contrast, in the hydroxyapatite-coated samples, correlation coefficients showed low values. Depth of bone penetration showed low correlation coefficients in both hydroxyapatite-coated and uncoated samples.

4. Discussion

Hydroxyapatite has been proposed as a coating material for titanium porous prosthetic implants in order to improve bone ingrowth. However, different factors have been observed to affect bone formation near and within the porous layer. The present experiment was designed to study the effect of hydroxyapatite coating while isolating other factors. Intramedullar and transcortical implantation methods have been proposed in previous studies for the evaluation of bioceramic-coated implants in animal models [3, 11–15]. Intramedullar cancellous bone implantation was chosen in the present work to investigate the potential benefit of coating with hydroxyapatite, because the transcortical model is less similar to the actual implantation of uncemented prostheses. Values of shear strength at the bone–implant interface seem to be related to the time since implantation, and to the type of porous coating used. Implant loading and its initial stability may also influence subsequent fixation strength. For these reasons, results tend to vary, depending on implant de-

sign, model used, and the associated experimental conditions. Thus, Cook *et al.* [12, 13], reported an insignificant increase of the attachment strength when comparing hydroxyapatite-coated and uncoated porous titanium canine implants at 3, 6 and 12 weeks; Oonishi *et al.* [15] found four times greater bonding strength in hydroxyapatite-coated than in uncoated porous titanium samples at 2 weeks and two times greater at 6 weeks. At 12 weeks, results were similar. Galante and Rivero [3] and Rivero *et al.* [17], examined plasma-sprayed hydroxyapatite coatings applied to titanium fibre metal transcortical and intramedullar implants, and reported a significantly greater mean attachment strength after 4 weeks implantation, but no attempt was made to compare the data based on the implantation type. Samples tested after 1, 2 or 6 weeks exhibited no significant differences between hydroxyapatite-coated and uncoated samples, although in each case the hydroxyapatite-coated strength was slightly greater. Recently, Cook *et al.* [11] reported a stronger interface between hydroxyapatite and bone than between titanium and bone in a transcortical non-porous model at 5, 10 and 32 weeks. Therefore, existing results are controversial, and it is still difficult to assess the true value of hydroxyapatite coating in porous implants.

In the present study, the low cancellous bone shear strength may explain the lack of differences in push-out tests between hydroxyapatite-coated and uncoated specimens, in spite of the fact that more bone ingrowth was found in the hydroxyapatite-coated sides. The present ultimate shear stress obtained from test specimens is compatible with the mean shear strength of cancellous bone (6.60 + 1.66 MPa) as reported by Carter and Hayes [18] and Stone *et al.* [19] Therefore, the bone–implant interface strength is at least as strong as the cancellous bone, independently of the implant coating type. This assumption was further supported by the predominance of trabecular fractures revealed from the microradiographs of the push-out specimens. As suggested by Oonishi *et al.* [15], it is possible that at 12 weeks, hydroxyapatite-coated and uncoated implants had an interface shear strength significant higher than the trabeculae surrounding the implant. The morphological evaluations for porosity, bone ingrowth and bone ongrowth were performed on BEI-SEM micrographs in order to improve the accuracy of measurement compared to microradiographic techniques [20, 21].

Microradiography shows fine details of the trabecular shape but overestimates ingrowth and underestimates porosity because the evaluation is based on a projected view of a specimen with certain thickness. This fact is well known in histology and is termed the Holmes effect [22]. The BEI-SEM method is considered superior since a slice thickness of only 1–5 μm on the surface of the specimen is studied, thus eliminating the projection or Holmes effect [23]. In contrast, morphological evaluation of the failure mechanism of the push-out samples was performed by the microradiographs because the BEI-SEM sections are too thin to analyse the trabeculae rupture and debonding patterns. BEI-SEM images revealed that the hydroxyapatite-coated specimens of both groups achieved bone mineralization directly linked to the coating surface. The mushroom-like trabeculae patterns in hydroxyapatite-coated specimens were the result of an osteoconductive effect on the surface of hydroxyapatite-coated beads. Strong bonding between bone and hydroxyapatite was demonstrated by the morphological evidence of the pushed-out samples, which failed to reveal any debonding failures at the hydroxyapatite–bone interface. This finding suggests the existence of a direct bonding between bone and hydroxyapatite as previously reported [24]. Such results were also found by Cook *et al.* [12, 13]. In contrast, the arc-shaped trabeculae formation observed in the uncoated samples of both groups was the result of a lack of direct bone apposition on the titanium surface. The histomorphometric data suggest that the hydroxyapatite coating was an effective method to improve bone formation and ingrowth in the porous prosthesis to enhance stable biological fixation. A strong correlation between bone ingrowth and push-out interface strength was observed in the uncoated titanium implants. On the other hand, in the hydroxyapatite-coated implants, the values of the correlation coefficients were very low. This fact suggested that hydroxyapatite can play a major role in the definition of the interface strength. These results support the clinical relevance of the principles involved in the hydroxyapatite coating of titanium porous-coated uncemented prostheses.

Acknowledgements

The authors would like to thank Fred Schultz for designing instruments for implant insertion and specimen cutting, Lawrence Berglund for push-out test realization, "Area di Ricerca Corrente 5" of the Rizzoli Institute for partial funding and the equal contribution by the Mayo Foundation.

References

1. M B COVENTRY, in "Joint replacement arthroplasty" (Churchill Livingstone, New York, 1991) p. 491.
2. C. A. ENGH, *Clin. Orthop.* **176** (1983) 52.
3. J. O GALANTE and D. P. RIVERO, in "Advanced concepts in total hip replacement" (W. H. Harris, Thorofare: Slack, 1985) p. 135.
4. J. P COLLIER, M. B MAYOR, J. C CHAE, V. A SURPRENANT, H. P. SURPRENANT and L. A. DAUPHINAIS, *Clin.Orthop.* **235** (1988) 173.
5. S. D. COOK, K. A. THOMAS and R. J HADDAD, *ibid.* **234** (1988) 90.
6. R. JUDET, M SIGUIER, B. BRUMPT and TH JUDET, *Rev. Chir. Orthop.* **64** (Suppl. 2) (1978) 14.
7. G. A. LORD, J. R. HARDY and F. J. KUMMER, *Clin. Orthop.* **141** (1979) 2.
8. H. MITTELMEIER and G HARMS, *Z. Orthop.* **117** (1979) 478.
9. B. M TRACY and R H DOREMUS, *J. Biomed. Mater. Res.* **18** (1984) 719.
10. R. G T. GEESINK, *Clin. Orthop.* **261** (1990) 39.
11. S. D COOK, K A. THOMAS and J. F. KAY, *ibid.* **265** (1991) 280.
12. S. D. COOK, K A. THOMAS, J. F. KAY and M J. JARCHO, *ibid.* **230** (1988) 303.
13. S. D COOK, K. A. THOMAS, J F. KAY and M J. JARCHO, *ibid.* **232** (1988) 225.

14. R. G. T. GEESINK, K. de GROOT and C. P. A. T. KLEIN, *J. Bone Joint Surg.* **70-B** (1988) 17.
15. H. OONISHI, M. YAMAMOTO, H. ISHIMARU, E. TSUJI, S. KUSHITANI, M AONO and Y. UKON, *ibid.* **71-B** (1989) 213.
16. D R. SUMNER, D. P. RIVERO, A. K. SKIPOR and J. O. GALANTE, *Trans. Soc. Biomater.* **9** (1986) 69.
17. D. P. RIVERO, J. FOX, A. K. SKIPOR, R. M. URBAN and J. O. GALANTE, *J. Biomed. Mater. Res.* **22** (1988) 191.
18. D. R. CARTER and W. C. HAYES, *J. Bone Joint Surg.* **59-A** (1977) 954.
19. J. L. STONE, G. S. BEAUPRE and W. C. HAYES, *J. Biomech.* **16** (1983) 743.
20. R. D. BLOEBAUM, K. N. BACHUS and T. M BOYCE, *J. Biomater. Appl.* **5** (1990) 56.
21. D. R SUMNER, J. M. BRYAN, R. M. URBAN and J. R. KUSZAC, *J. Orthop. Res.* **8** (1990) 448.
22. W. J. WHITEHOUSE, *J Microsc.* **107** (1976) 183.
23. R. E. HOLMES, H. K. HAGLER and C. A. COLETTA, *J. Biomed. Mater. Res.* **21** (1987) 731.
24. K. A. THOMAS, J. F. KAY, S. D. COOK and M J JARCHO, *ibid.* **21** (1987) 1395.